



Research Article

# Optimization and biosynthesis of calcined chicken eggshell doped titanium dioxide photocatalyst based nanoparticles for wastewater treatment

Tafere Aga Bullo<sup>1</sup> · Yigezu Mekonnen Bayisa<sup>1</sup>  · Mohammed Seid Bultum<sup>1</sup>

Received: 13 August 2021 / Accepted: 26 November 2021

Published online: 11 December 2021

© The Author(s) 2021 [OPEN](#)

## Abstract

This study presents, biosynthesis of calcinated eggshell (CES) doped with Titanium dioxide ( $\text{TiO}_2$ ) photocatalyst for photodegradation of methylene blue from synthetic wastewater. The influence of three independent variables for improving photodegradation efficiency was investigated and optimized using response surface methodology of Box–Behnken Design on the removal of methylene blue using the calcined chicken eggshells (CES) doped with titanium dioxide. The experimental result showed that 95.8% degradation efficiency of methylene blue by prepared photocatalyst at a contact time of 180 min, initial concentration of methylene blue of 10 ppm, and calcined eggshells (CES) doped with titanium dioxide dose of 2.5 g/L. The synthesized photocatalyst was characterized by Fourier-transform infrared spectroscopy, UV-spectrometer, and X-ray diffractometer and UV–vis Spectroscopy for determined their functional group, structure, and bandgap energy respectively. Their results depict the calcined eggshell doped with titanium dioxide photocatalyst is a promising option for the degradation of methylene blue from industrial wastewater under the stated condition.

## Highlights

- Analysis of chicken eggshell wastes are being used as photocatalyst source to calcinated eggshell doped  $\text{TiO}_2$ , i.e., ‘Waste to photocatalyst’ for production of viable sustainable products to bio photocatalyst from wastewater to fulfill the need of an expensive metal-doped catalyst.
- Photocatalytic degradation of Methylene Blue experiment has been done.
- The highest degradation efficiency of 95.8% methylene blue was obtained at a contact time of 180 min, 10 ppm of initial concentration of methylene blue, and a dopant dose of 2.5 g/L by using prepared photocatalyst.

**Keywords** Calcinating eggshell · Calcined eggshell doped titanium dioxide · Photocatalyst · Wastewater treatment

## 1 Introduction

Now a day, the health problem connected with water pollution is the major and primary issue throughout the world [1]. The main cause of water pollution is directly and indirectly related to man-made activities that lead

to the poor control of wastewater. The focal sources of wastewater is consequently due to the weak controlling mechanism of wastes from the industrial activity plus humans, animals, household, and laundry sludge might be due to the lack of treatment services, or the fact that the existing facilities are not functioning as intended and

✉ Yigezu Mekonnen Bayisa, yigezu338@gmail.com | <sup>1</sup>School of Chemical Engineering, Jimma Institute of Technology, Jimma University, Jimma, Oromia, Ethiopia.



has led to extensive environmental pollution [2]. On the other hand, utilizing this untreated wastewater in agricultural activities led to risk for both farmers who have a connection through this water and crop consumers via transfer of pathogenic microorganisms (microbes that cause disease) from water to crop. In addition to this, pathogenic aquatic diseases like cholera, enteric fever, diarrhea, and dysentery are caused by the exploitation of this untreated wastewater that can be spread through drinking water [3, 4].

Besides an indicator of country's economic improvement, rapid industrialization are greatly associated with environmental degradation, mainly due to the discharge of untreated wastewater or partially treated wastewater [5]. In addition to this, in developing country most of the industries discharge wastewater to near around water stream without adequate treatment due to the lack of know-how, low-profit margins, failure to afford investment costs in pollution remediation equipment and technologies, and financial support [6]. Those who have better capital are not willing to install efficient treatment technologies, due to lack of governmental control and weak implementation of environmental policies in the country [7]. Therefore, there is an urgent need towards providing a wastewater treatment option for these industries to allow environmentally friendly disposal of their wastewater that reaches specific effluent quality goals [8].

There are several available methods for the exploitation and purification of wastewater in order to reduce their effects on the environment. Accordingly, there is a strong need to develop novel bio-based product from cheaper, available resources and renewable feedstock, which played a pivotal role in wastewater purification, particularly photocatalytic activity of doped titanium dioxide ( $\text{TiO}_2$ ) deliberately used to remove contaminants from wastewater [9, 10]. Titanium dioxide is the most common photocatalytic with the best performance, low price, and toxicity. Titanium dioxide is a quite versatile catalyst that can absorb UV light that is applied in many different situations and is capable of handling many different forms and amounts of organic waste [11]. There are different metal or nonmetal ion-doped with  $\text{TiO}_2$  such as B, C, N,  $\text{Fe}^{3+}$ ,  $\text{CO}_3^{2-}$ , and  $\text{Zn}^{2+}$  that used to increase light absorption of  $\text{TiO}_2$  from UV to the visible range [12]. For instance, coupling  $\text{TiO}_2$  with  $\text{CO}_3^{2-}$  ion improves the capability of the catalyst, increases the light absorption band energy of  $\text{TiO}_2$  and increases the photocatalytic activity of  $\text{TiO}_2$  under solar irradiation [13, 14]. The  $\text{TiO}_2$ - $\text{CaCO}_3$  can be created through the surface hydroxyl group in the liquid phase system at the interface of a phase of  $\text{CaCO}_3$  and  $\text{TiO}_2$ , since  $\text{CO}_3^{2-}$  is generated in-situ on the catalyst surface [14].

The  $\text{CO}_3^{2-}$  ion that can be used to enhance the photocatalytic activity of  $\text{TiO}_2$  can be derived from different biomass rich in  $\text{CaCO}_3$ . Poultry eggs biomass (eggshells) contain 94–97 wt. %  $\text{CaCO}_3$ . Hence, due to its randomized porous structure, locally available, waste resources, eco-friendliness, low cost, and nontoxicity can be used as a carrier for nano-biomass. Synthesizing calcined chicken eggshell doped  $\text{TiO}_2$  photocatalysts with a porous structure generate  $\text{CO}_3^{2-}$  species can be for methylene blue degradation under light illumination [15, 16].

The present study puts forward a synthesis of effective photocatalyst of calcined chicken eggshell doped  $\text{TiO}_2$  for the degradation of methylene blue under solar light irradiation. Moreover, the possible degradation pathway is proposed and the photocatalytic mechanism of methylene blue degradation over calcinated chicken eggshell is confirmed. Response surface methodology (RSM) is applied to optimize the reaction conditions and further evaluate the interaction among the selected process parameters.

## 2 Materials and methods

### 2.1 Materials and reagents

All reagents that used in this study were pure analytical grade. The methylene blue ( $\text{C}_{27}\text{H}_{37}\text{N}_3\text{ClS}_3$  with a molecular weight of 319.85 g/mol) was purchased from Chem-Supply Kirkos Ltd. in Addis Ababa, Ethiopia. The photocatalyst employed was commercially 98% titanium dioxide ( $\text{TiO}_2$ ) produced by Loba Chemicals Pvt. Ltd in India was purchased from Atomic Educational Materials Supply PLC in Addis Ababa.  $\text{NH}_4\text{OH}$  and HCL were used for pH adjustments. Chicken eggshells were collected from Jimma University Institute of Technology staff launches.

### 2.2 Synthesis of calcined egg shells (CES)

To prepare chicken eggshell powder first chicken eggshells were collected from Jimma University Institute of Technology staff launches, and soaked in hot water for 5–10 min and washed with tap water repeatedly to remove any impurities. The shells were dried in an oven at 105 °C for 12 h. Finally, the dried shells were crushed to a uniform size by selecting the powder using a sieve of 200 meshes. The crushed eggshell powder was put into an alumina crucible and calcined in a muffle furnace at 1000 °C temperatures for 1 h $\frac{1}{2}$ . The resulting powder material was washed with distilled water and dried at 105 °C for 12 h, then calcinated at a rate of 2 °C/min till attain 400 °C and kept at this temperature for 4 h. Finally, the product called Calcined Egg Shells (CES) was collected in a glass bottle.

## 2.3 Preparation of calcined egg shells doped titanium dioxide

The equal proportion mixture of  $\text{TiO}_2$  and Calcined Egg Shells (CES) was introduced into a vessel equipped with a stirrer. The homogenization of the two mixtures was carried out by adding a small amount of distilled water. The solution was concentrated by removing the water and heated in a  $105^\circ\text{C}$  oven for 12 h and the sample was dried. The homogenized fine powder material was obtained and calcined at  $400^\circ\text{C}$  for 4 h [16]. Then distilled water was used to wash the obtained product powder. Finally, a product called Calcined Egg Shells (CES) doped  $\text{TiO}_2$  was dried and characterized.

## 2.4 Characterization techniques

Calcined Egg Shells and Calcined Egg Shells (CES) doped  $\text{TiO}_2$  catalysts were characterized by using an X-ray diffractometer (XRD-7000) and a Fourier Transform Infrared (FTIR) spectroscopy Nicolet model Protégé 460 Magna IR spectrometer. FTIR spectroscopy was used to identify organic and inorganic compounds present in the photocatalyst. The Fourier transform infrared spectroscopy, FTIR (Perkin Elmer, Ettlingen, Germany) was used to confirm the functional groups in the synthesized photocatalyst of CES doped with  $\text{TiO}_2$  with the help of IR correlation charts, and the spectra were recorded in the range of wavenumber from  $4000$  to  $400\text{ cm}^{-1}$ . To approve the effective synthesis of CES doped with  $\text{TiO}_2$ , the XRD analysis for the crystal structure of the photocatalysts was investigated using a Darwell XRD 7000, with  $\text{K}\alpha$  (3 kW) x-ray diffractometer. The analysis was conducted in a range of  $10$ – $80^\circ$  at a scanning speed of  $2$ -degree  $\text{min}^{-1}$ . The degradation of methylene blue test and optical properties were determined using SPECORD 200 Plus UV–vis spectroscopy (Analyticjena, AG, and Germany). The UV–visible spectroscopy analysis for identifying the maximum wavelength by dissolving photocatalysts in ethanol using a water–ethanol mixture as a baseline. Then, those wavelengths were used to calculate the band gap of both photocatalysts.

## 2.5 Photocatalytic degradation of methylene Blue

To evaluate photocatalytic degradation of methylene blue, the synthesized Calcined Egg Shells doped  $\text{TiO}_2$  was added to the prepared synthetic methylene blue solution in a photoreactor equipped with a magnetic stirrer, pH meter, a thermometer, 9 W LED lamp at a distance of 10 cm, and water bath. Then, the desorption of the Methylene blue from the surface of the Calcined Egg Shells doped  $\text{TiO}_2$  catalyst was achieved by modification of the solution pH. The catalyst was removed by centrifugation at 3500 rpm.

## 2.6 Experimental design

The degradation efficiency of the Calcined Eggshell doped  $\text{TiO}_2$  photocatalyst on the removal of methylene blue was analyzed by using Design-Expert software version 13.0.5.0. Response Surface Methodology of Box-Behnken Design (BBD) three-level which consisted of 15 randomized experimental runs was used to determine the effects of photodegradation on the removal of methylene blue. The independent variables namely concentration of methylene blue (100–300 ppm), a dosage of CES doped  $\text{TiO}_2$  (0.5–2.5 g/L), and degradation time (60–180 min), and dependent variable as degradation of methylene blue were investigated. The degradation efficiency of the Calcined Eggshell doped  $\text{TiO}_2$  photocatalyst ( $Y$ ) was measured according to Eq. 1.

$$\text{Degradation efficiency, } Y(\%) = \frac{C_{MBO} - C_{MB}}{C_{MBO}} * 100 \quad (1)$$

where,  $C_{MBO}$  is the initial concentration of MB and  $C_{MB}$  is the concentration of MB at the time of sampling.

## 3 Results and discussion

### 3.1 Analysis of photocatalyst

The photocatalyst of CES doped titanium dioxide was characterized by FT-IR, XRD, and UV–vis Spectroscopy analysis for determination of their functional group, structure, and bandgap energy respectively. There result is shown in Figs. 1, 2 and 3.

As it is shown in Fig. 1a Fourier Transform Infrared (FTIR) spectroscopy determined the highest peak at  $3500\text{ cm}^{-1}$  and the lowest peak at around  $3125\text{ cm}^{-1}$  which depicts that they are both in the single bond region in the photocatalytic of Calcined Eggshell doped  $\text{TiO}_2$ . A slightly broad peak around the wavenumber of  $3500\text{ cm}^{-1}$  was attributed for the OH stretch bond, which illustrates the existence of alcohol and phenols; while at  $3125\text{ cm}^{-1}$  there was a C–H stretch bond that shows the existence of an aromatic ring. The peaks of bending vibration at  $1640\text{ cm}^{-1}$  were attributed to alcohol and phenols due to chemisorbed or physisorbed moisture on the surface of Calcined Eggshell doped  $\text{TiO}_2$  nanoparticles show an O–H stretch and free hydroxyl bond [12, 15]. The peaks around  $680$ – $610\text{ cm}^{-1}$  show the presence of an  $\text{SO}_4^{2-}$  group. After Calcined Eggshell was doped with  $\text{TiO}_2$  there was the disappearance of the region around  $2920\text{ cm}^{-1}$  and formation peaks bending vibration between  $1100$  and  $900\text{ cm}^{-1}$ . In this study, Fourier Transform Infrared (FTIR) spectroscopy

**Fig. 1** Fourier Transform Infrared spectra of **a** Calcined chicken eggshell doped  $\text{TiO}_2$  **b** pure Calcined chicken eggshell

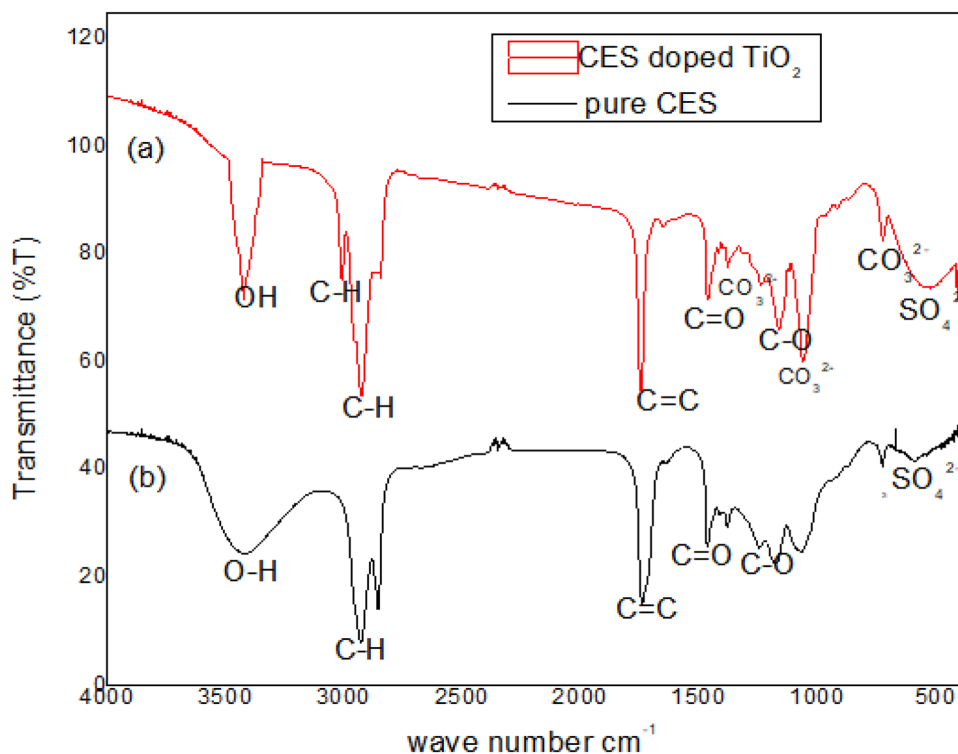
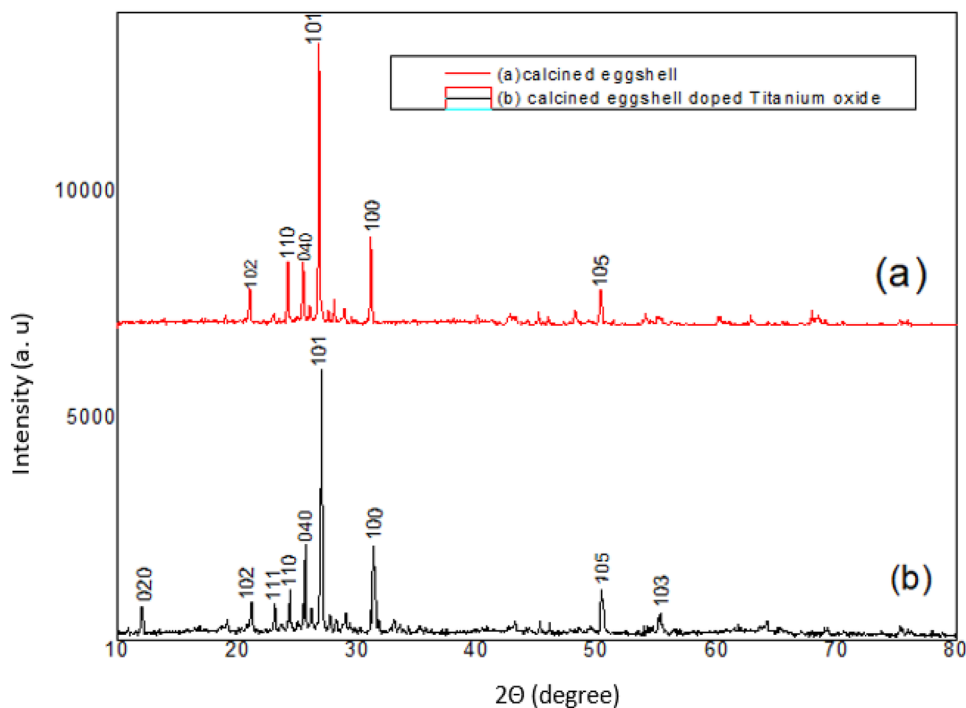


**Fig. 2** X-ray diffraction patterns of **a** calcined eggshell **b** calcined eggshell doped Titanium oxide



successfully confirmed that carbonate group was attributed around the peak at  $1400, 870, \text{ and } 710 \text{ cm}^{-1}$ .

Figure 1b showed that the presence of a functional group of different compounds found in pure Calcined Eggshell in the range of  $400\text{--}4000 \text{ cm}^{-1}$ . Thus, the band observed between  $3650 \text{ and } 3120 \text{ cm}^{-1}$  associated with

the hydroxyl (OH) and carbonyl functional group respectively while the weak bands at the region of  $2920 \text{ cm}^{-1}$  dispensed to asymmetric C–H stretching. On the other hand, the peak observed in the region between  $1700 \text{ cm}^{-1}$  and  $1490 \text{ cm}^{-1}$  were assigned to C=C of pyrone and C=O of carboxylic groups correspondingly.

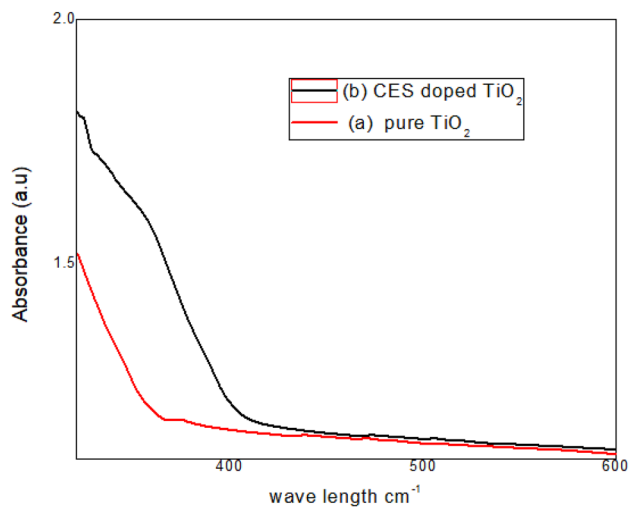


**Fig. 3** Ultraviolet-Visible spectra of **a** pure  $\text{TiO}_2$  **b** calcined eggshell doped  $\text{TiO}_2$

In addition to this, the functional group of C–O present in compounds like carbonyls, ketones, aldehydes, or ester groups were observed peak at  $1632\text{ cm}^{-1}$  in the aromatic region [9, 17]. The peak in the range of  $1200\text{--}900\text{ cm}^{-1}$  has also been associated with either Si–O or C–O stretching in alcohol and ether.

The XRD analysis was conducted for both Calcined chicken eggshell (CES) and Calcined chicken eggshell (CES) doped  $\text{TiO}_2$  photocatalyst. XRD was used to confirm the formation of CES doped  $\text{TiO}_2$  nanoparticles prepared used for methylene blue water extract.

The XRD pattern for both CES and CES doped  $\text{TiO}_2$  is shown in Fig. 2a, b respectively. The X-ray diffraction pattern of calcined chicken eggshell doped  $\text{TiO}_2$  peaks observed at  $2\theta = 12.01^\circ, 21.19^\circ, 23.11^\circ, 24.34^\circ, 25.57^\circ, 26.89^\circ, 31.2^\circ, 50.32^\circ,$  and  $55.3^\circ$ , correspond to miller indices (020), (102), (110), (111), (040), (101), (100), (105), and (103) respectively (JCPDS card:19- 2403) which associated to anatase phase of titania whereas Calcined chicken eggshell major peak observed at  $2\theta = 21.04^\circ, 24.19^\circ, 25.48^\circ, 26.8^\circ, 31.12^\circ,$  and  $50.26^\circ$  correspond to the reflection planes of (102), (110), (040), (101), (100), and (105) which confirm the presence of well-crystallized pure anatase phase. The peak at  $2\theta = 26.8^\circ$  is attributed to anatase phase CES while the peak at  $50.26^\circ$  shows the presence of the brookite phase [16]. The other peak at  $2\theta = 12.01^\circ$  indicates that orthorhombic titania phase presented in Calcined chicken eggshell doped  $\text{TiO}_2$  in the recorded peaks [15]. The reason for the newly emerged peaks in the CES doped  $\text{TiO}_2$  is given to calcination the process of doping the photocatalyst. The average crystallite size of the nanoparticles was calculated using Debye–Scherer's Equation [18, 19].

$$D = \frac{k\lambda}{\beta\cos\theta} \quad (2)$$

where  $D$  is the crystallite size of CES doped  $\text{TiO}_2$  in nm,  $K$  is the Scherrer shape factor (0.90),  $\lambda$  is the X-ray wavelength used ( $1.5406\text{ \AA}$ ),  $\beta$  is the full width at half maximum in radians and,  $\theta$  is the Bragg diffraction angle in degrees. Thus, the average particle sizes of CES and CES doped  $\text{TiO}_2$  were predicted as 15 and 17.4 nm correspondingly. The variance in sizes could be happened during the impregnation process compared to the CES doped  $\text{TiO}_2$ .

Figure 3 reports the Ultraviolet-Visible absorbance spectra in terms of absorbance of  $\text{TiO}_2$  and CES doped  $\text{TiO}_2$ . As it has shown in Fig. 3 the shifting of the absorption onset from about 387 nm (for undoped  $\text{TiO}_2$ ) to about 449 nm (for CES doped  $\text{TiO}_2$ ) indicates the ability of the sample to absorb visible light. The bandgap energies of pure  $\text{TiO}_2$  and obtained calcined eggshell doped  $\text{TiO}_2$  with the wavelength from UV-Vis absorption spectra were calculated using Eq. 3 [20].

$$\text{Band gap}(eV) = \frac{1240}{\text{wavelength}(nm)} \quad (3)$$

As observed from the result, the typical optical band gap energy values of incorporating Calcined chicken eggshell into  $\text{TiO}_2$  indicates that a decreasing of the unnecessary bandgap. Therefore, the band gap has lowered from 3.2 eV to 2.76 eV. This result is associated with the shielding the outward of  $\text{TiO}_2$  by deposition of the carbonated ion of Calcined chicken eggshell catalyst which leads to minimizing the effective surface area of absorbing light.

Analysis variances of photocatalytic degradation of methylene blue.

Based on the analysis of variance (ANOVA) the parameter which significantly affected the degradation efficiency of methylene blue was shown in Table 1. From this table, the Model F-value of 331.86 implies the model is significant,  $P$ -values less than 0.0500 indicate model terms and all factors are significant and the Lack of Fit F-value of 1.47 implies the Lack of Fit is not significant.

### 3.2 Variables effect on the degradation efficiency of methylene blue

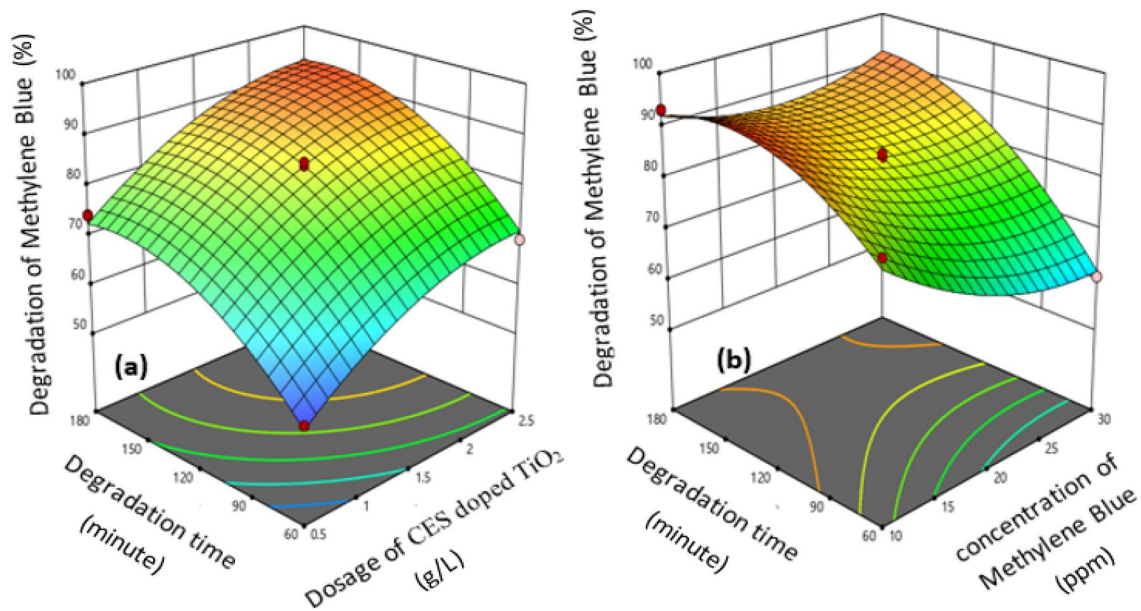
The response surface curves representing the parameter effects of three variables, i.e., a dosage of CES/ $\text{TiO}_2$ , initial concentration of methylene blue, degradation or treatment time on methylene blue degradation compounds by CES/ $\text{TiO}_2$  photocatalyst were investigated.

Figure 4a shows that a maximum methylene blue degradation was attained at a high treatment time and a considerably low initial concentration of methylene blue. Increasing the photocatalyst dosage from 0.5 g/L to 2.5 g/L



**Table 1** ANOVA analysis for process parameter

Sources	Sum of the squares	Sum of the mean	F-value	P-value	
Model	2161.92	240.21	331.86	< 0.0001	Significant
A-dosage of CES doped TiO <sub>2</sub>	595.47	595.47	822.66	< 0.0001	
B-concentration of MB	260.60	260.60	360.03	< 0.0001	
C-degradation time	901.43	901.43	1245.35	< 0.0001	
AB	0.0676	0.0676	0.0934	0.7722	
AC	0.1369	0.1369	0.1891	0.6818	
BC	84.09	84.09	116.17	0.0001	
Residual	3.62	0.7238			
Lack of Fit	2.49	0.8308	1.47	0.4285	Not significant

**Fig. 4** Effect of process parameter on the degradation efficiency of methylene blue (%)

also increased the degradation efficiency. But, the later increase in degradation was smaller in range compared to the first showing that the effect of photocatalyst concentration on the degradation efficiency has slowed down. This is because the increased amount of photocatalyst blocks the light from reaching some of the particles which makes some of the photocatalysts surfaces unavailable for light absorption, which indicated that it has approached the optimum concentration of photocatalyst [16, 21, 22].

The initial concentration of methylene blue during the treatment process was significantly affecting the efficiency of photocatalytic degradation. As shown in Fig. 4a increasing the methylene blue concentration from 10 to 30 ppm the degradation efficiency of photocatalytic calcinated eggshell doped with titanium dioxide was decreased i.e., a small amount of it can be adsorbed on the surface of the photo-catalyst at higher concentration. On the other hand,

a maximum methylene blue degradation was obtained at a relatively high dosage dopant and low initial concentration of methylene blue [23, 24]. In addition to this, after three hours of UV irradiation, the degradation yields of methylene blue concentration at 10, 20, and 30 ppm were about 95.8%, 84.8%, and 60.7%, respectively.

In this work efficiency of the photocatalytic calcinated eggshell doped with TiO<sub>2</sub> and contact time were significantly affected adsorption of methylene blue degradation was presented in Fig. 4b. As it can see in this figure the degradation efficiency of MB is directly proportional to the time spent in the degradation process. The sudden increase in degradation efficiency in the 180 min is attributed to the effect of the higher dopant dosage of a photocatalyst. A higher dosage of photocatalyst has an effect because a higher dosage means it takes a longer time to react to start an efficient degradation process. And also due to the complex structure of the

pollutant, methylene blue takes a longer time to reach full degradation [25, 26]. In general, at sufficient contact time and low initial concentration the increment in dopant dose from 0.5 to 2.5 g/L results in an increment of methylene blue degradation efficiency from 52.5% to 95.8%.

### 3.3 Optimization of methylene blue degradation efficiency

The program randomly picks a set of conditions from which to start its search for desirable results was indicated as the ramps function in Fig. 5. The colored dot on each ramp reflects optimum values of the factors and response. Thus, the red colors indicated that the value at which the optimum value of methylene blue degradation (blue color) was obtained. The Design-Expert sorts the results from most desirable to least as it shown in Figs. 6. This depicts that the desirability results were indicated as the ramps function for the optimization of three factors (dosage of calcined eggshell/TiO<sub>2</sub>, concentration of MB, and degradation time) to yield the maximum removal (%) efficiency of methylene blue. The predicted R<sup>2</sup> implies that an error value, used to estimate the value of the current model and sum of squares is defined by the total squares, and the numerical value differs between 0 and 1. The higher the validity of the proposed model, when the number is closer to one. The value of R-squared in this study was equal to 0.9983 and shows the strength and high adaptability of the proposed model for the removal of methylene blue by the calcined

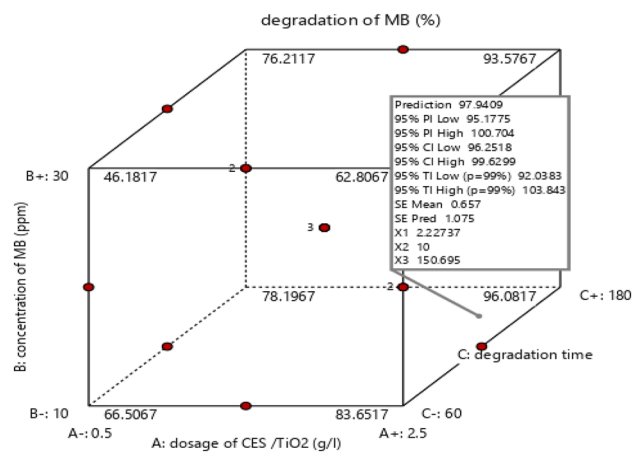


Fig. 6 Optimization of methylene blue degradation efficiency

eggshell doped with TiO<sub>2</sub> photocatalytic process. The points at which the maximum desirability and effects all factors on methylene blue degradation efficiency were indicated in Fig. 7. As shown in Fig. 7, the maximum removal of 97.9409% was obtained at a maximum level of the initial methylene blue concentration of 30 g/L, adsorbent dose of 2.5 g/L, and contact time of 180 min, with methylene blue desirability of one. Thus, the predicted run of the optimum degradation efficiency of methylene blue was selected which is higher in desirability (0.863) than others observed from constraints solution.

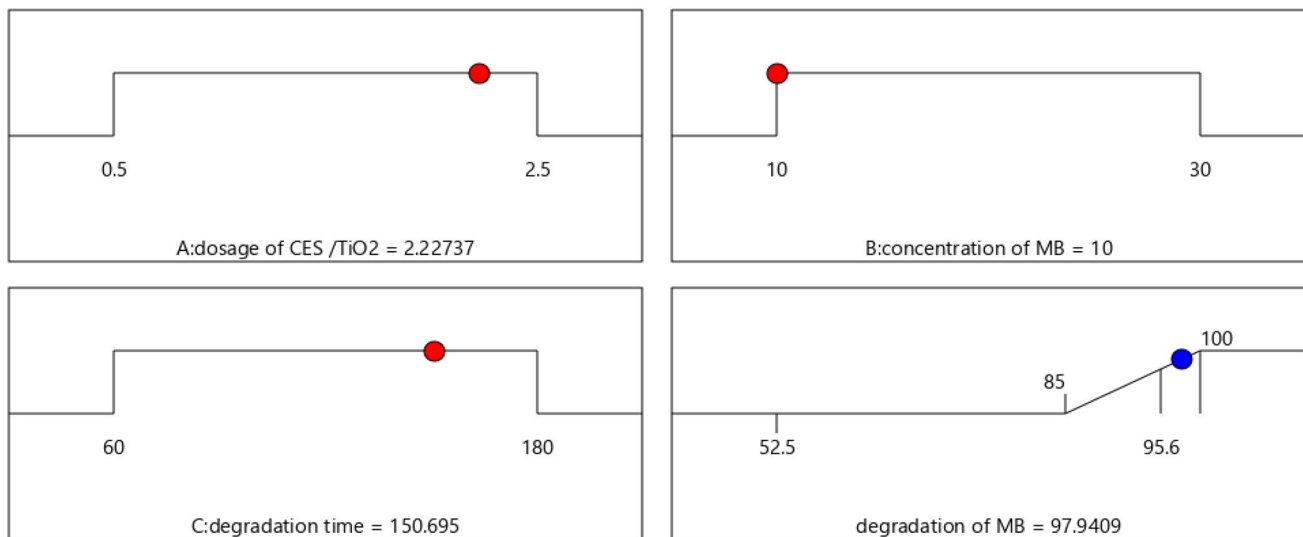


Fig. 5 Numerical Optimization Ramps (red colors for optimum value of factors and blue color for optimum value of methylene blue degradation)

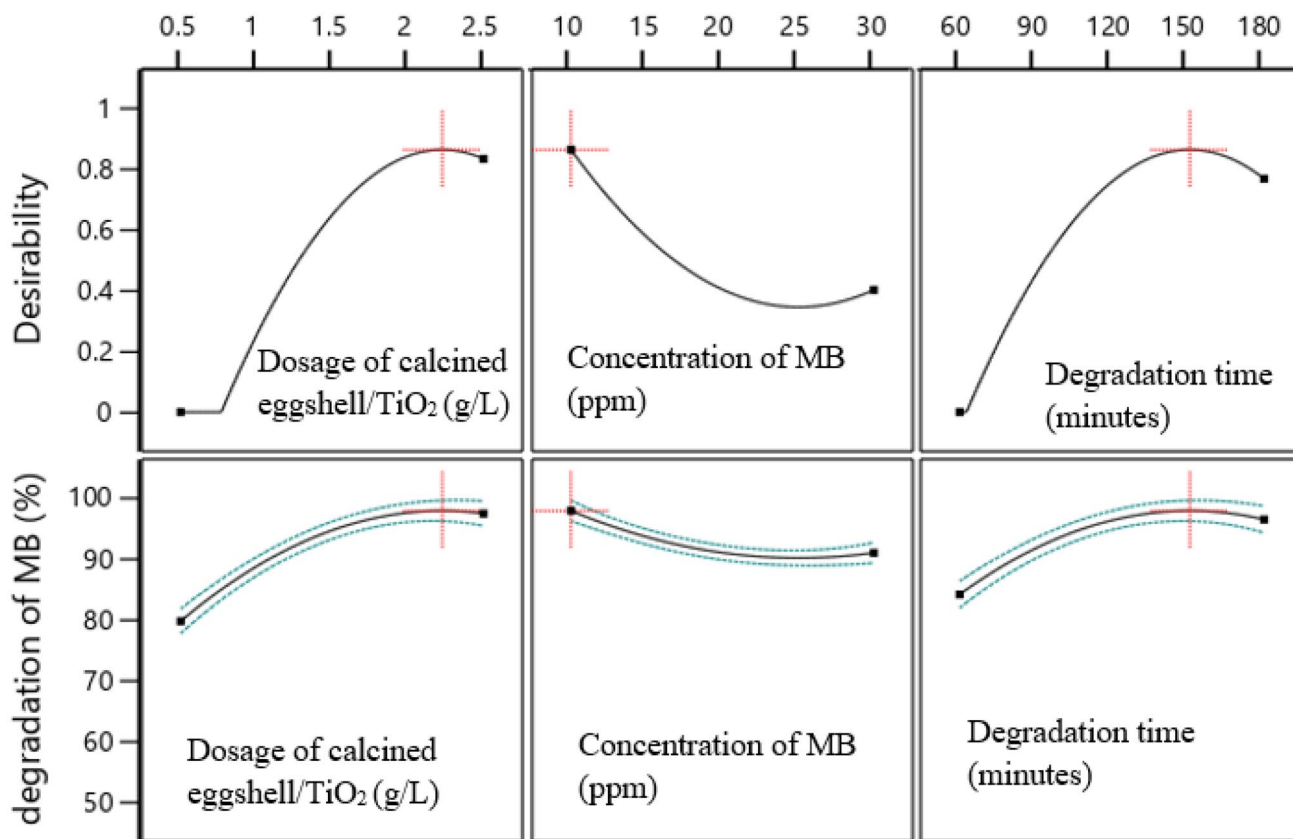


Fig. 7 Constrain solution of desirability and effects of all factors on optimum methylene blue degradation

### 4 Conclusion

In this study Calcine Eggshell doped titanium dioxide was investigated for degradation of methylene blue compound from industrial wastewater. The prepared Calcine Eggshell doped titanium dioxide photocatalyst of functional group, structure, and bandgap energy was characterized by FT-IR, XRD, and UV-vis Spectroscopy analysis for respectively. The result of the study shows that calcinated eggshell dopant is a good photocatalyst for degradation of methylene blue from wastewater decontamination due to the presence of potential binding sites and functional groups which confirm the degradation process. The prepared photocatalyst showed that 95.8% degradation efficiency of methylene blue was obtained at a contact time of 180 min, 10 ppm of initial concentration of methylene blue, and a dopant dose of 2.5 g/L. Therefore, the degradation process of degrading methylene blue compounds using calcinated eggshell doped titanium dioxide photocatalyst from wastewater can be used as a useful treatment process for methylene blue degradation. For future work further characterizations techniques such as scanning electron microscopy (SEM), transmission electron microscopy (TEM), and

energy-dispersive spectroscopy mapping (EDS-mapping will be done.

**Acknowledgements** We would like to acknowledge the XRD and FT-IR platform at the Faculty of Material Science and Engineering, Jimma University, and Jimma University for served internet-free.

**Data availability** Our data generated during the study are included in the manuscript.

### Declarations

**Conflict of interest** The authors declare that there is no conflict of interests regarding the publication of this article.

**Ethical approval** This article does not contain any studies with human participants or animals performed by any of the authors.

**Open Access** This article is licensed under a Creative Commons Attribution 4.0 International License, which permits use, sharing, adaptation, distribution and reproduction in any medium or format, as long as you give appropriate credit to the original author(s) and the source, provide a link to the Creative Commons licence, and indicate if changes were made. The images or other third party material in this article are included in the article's Creative Commons licence, unless indicated otherwise in a credit line to the material. If material is not included in the article's Creative Commons licence and your intended



use is not permitted by statutory regulation or exceeds the permitted use, you will need to obtain permission directly from the copyright holder. To view a copy of this licence, visit <http://creativecommons.org/licenses/by/4.0/>.

## References

1. Raizada P, Sudhaik A, Patial S, Hasija V, Parwaz Khan AA, Singh P et al (2020) Engineering nanostructures of CuO-based photocatalysts for water treatment: Current progress and future challenges. *Arab J Chem* 13(11):8424–8457. <https://doi.org/10.1016/j.arabjc.2020.06.031>
2. Yaqoob AA, Parveen T, Umar K (2020) Role of nanomaterials in the treatment of wastewater: a review. *Water* 12:495. <https://doi.org/10.3390/w12020495>
3. Liu S, Su Z-L, Liu Y, Yi L-Y, Chen Z-L, Liu Z-Z (2021) Mechanism and purification effect of photocatalytic wastewater treatment using graphene oxide-doped titanium dioxide composite nanomaterials. *Water* 13:1915. <https://doi.org/10.3390/w13141915>
4. Taylor P, Umar K, Dar AA, Haque MM, Mir NA, Muneer M (2012) Photocatalysed decolourization of two textile dye derivatives, martius yellow and acid blue 129, in UV irradiated aqueous suspensions of Titania. *Desalin Water Treat* 46(1–3):205–214. <https://doi.org/10.1080/19443994.2012.677527>
5. Alani OA, Ari HA, Alani SO, Offiong NO (1918) Visible-light-driven bio-templated magnetic copper oxide composite for heterogeneous photo-fenton degradation of tetracycline. *Water* 2021:13. <https://doi.org/10.3390/w13141918>
6. Umar K, Parveen T, Alam M, Mohamad MN (2019) Degradation of organic pollutants using metal-doped TiO<sub>2</sub> photocatalysts under visible light : a comparative study. *Desalin Water Treat*. <https://doi.org/10.5004/dwt.2019.24298>
7. Ngoepe NM, Mathipa MM, Hintsho-Mbita NC (2020) Biosynthesis of titanium dioxide nanoparticles for the photodegradation of dyes and removal of bacteria. *Optik (Stuttg)* 224:165728. <https://doi.org/10.1016/j.jijleo.2020.165728>
8. Shahmoradi B, Farahani F, Kohzadi S, Maleki A, Pordel M, Zand-salimi Y (2019) Application of cadmium-doped ZnO for the solar photocatalytic degradation of phenol. *Water Sci Technol* 79(2):375–385. <https://doi.org/10.1111/j.1551-2916.2008.02291.x>
9. Mustapha S, Ndamitso MM, Abdulkareem AS, Tijani JO, Shuaib DT, Ajala AO et al (2020) Application of TiO<sub>2</sub> and ZnO nanoparticles immobilized on clay in wastewater treatment: a review. *Appl Water Sci* 10:1–36. <https://doi.org/10.1007/s13201-019-1138-y>
10. Dong S, Feng J, Fan M, Pi Y, Hu L, Han X (2015) Recent developments in heterogeneous photocatalytic water treatment using visible light-responsive photocatalysts: A review. *RSC Adv* 5(19):14610–14630. <https://doi.org/10.1039/c4ra13734e>
11. Banerjee S, Benjwal P, Singh M, Kar KK (2018) Graphene oxide (rGO)-metal oxide (TiO<sub>2</sub>/Fe<sub>3</sub>O<sub>4</sub>) based nanocomposites for the removal of methylene blue. *Appl Surf Sci* 439:560–568. <https://doi.org/10.1016/j.apsusc.2018.01.085>
12. Al-Mamun MR, Kader S, Islam MS, Khan MZH (2019) Photocatalytic activity improvement and application of UV-TiO<sub>2</sub> photocatalysis in textile wastewater treatment: A review. *J Environ Chem Eng*. <https://doi.org/10.1016/j.jece.2019.103248>
13. Yang CC, Doong RA, Chen KF, Chen GS, Tsai YP (2018) The photocatalytic degradation of methylene blue by green semiconductor films that is induced by irradiation by a light-emitting diode and visible light. *J Air Waste Manag Assoc* 68(1):29–38. <https://doi.org/10.1080/10962247.2017.1358222>
14. Amarasinghe A, Wanniarachchi D (2019) Eco-Friendly photocatalyst derived from egg shell waste for dye degradation. *J Chem* 13:8184732. <https://doi.org/10.1155/2019/8184732>
15. Huang Z, Wang J, Yang MQ, Qian Q, Liu XP, Xiao L (2021) Construction of TiO<sub>2</sub>-eggshell for efficient degradation of tetracycline hydrochloride: Sunlight induced in-situ formation of carbonate radical. *Materials (Basel)* 14(7):1598
16. Echabbi F, Hamlich M, Harkati S, Jouali A, Tahiri S, Lazar S et al (2019) Photocatalytic degradation of methylene blue by the use of titanium-doped calcined mussel shells CMS/TiO<sub>2</sub>. *J Environ Chem Eng* 7(5):103293. <https://doi.org/10.1016/j.jece.2019.103293>
17. Khiavi ND, Katal R, Eshkalak SK, Masudy-Panah S, Ramakrishna S, Jiangyong H (2019) Visible light driven heterojunction photocatalyst of cuo-cu<sub>2</sub>o thin films for photocatalytic degradation of organic pollutants. *Nanomaterials* 9:1011. <https://doi.org/10.3390/nano9071011>
18. Hameed S, Siddiqui MJ, Haque MM (2014) Electrical and optical properties of nickel- and molybdenum-doped titanium dioxide nanoparticle: improved performance in dye-sensitized solar cells. *J Mater Eng Perform*. <https://doi.org/10.1007/s11665-014-0954-3>
19. Srivastava V, Pandey S, Mishra A, Kumar A (2019) Green synthesis of biogenic silver particles, process parameter optimization and application as photocatalyst in dye degradation. *SN Appl Sci* 1(12):1–15. <https://doi.org/10.1007/s42452-019-1762-z>
20. Umar K, Nasir M, Ibrahim M, Ahmad A (2019) Synthesis of Mn-doped TiO<sub>2</sub> by novel route and photocatalytic mineralization/intermediate studies. *Res Chem Intermed*. <https://doi.org/10.1007/s11164-019-03771-x>
21. Kumar A, Balouch A, Pathan AA, Muhammad A, Jagirani MS, Mustafai FA et al (2017) Remediation techniques applied for aqueous system contaminated by toxic chromium and nickel ion. *Geol Ecol Landscapes* 9508:1–11. <https://doi.org/10.1080/24749508.2017.1332860>
22. Mir NA, Khan A, Umar K, Muneer M (2013) Photocatalytic study of a xanthene dye derivative, phloxine B in aqueous suspension of TiO<sub>2</sub>: adsorption isotherm and decolourization kinetics. *Energy Environ Focus* 2(1):208–216
23. Sohrabi S, Akhlaghian F (2016) Modeling and optimization of phenol degradation over copper-doped titanium dioxide photocatalyst using response surface methodology. *Process Saf Environ Prot* 99:120–128. <https://doi.org/10.1016/j.psep.2015.10.016>
24. Xu Q, Wang Y, Chi M, Hu W, Zhang N, He W (2020) Porous polymer-titanium dioxide/copper composite with improved photocatalytic activity toward degradation of organic pollutants in wastewater: Fabrication and characterization as well as photocatalytic activity evaluation. *Catalysts* 10:310. <https://doi.org/10.3390/catal10030310>
25. Lazar MA, Varghese S, Nair SS (2012) Photocatalytic water treatment by titanium dioxide: Recent updates. *Catalysts* 2:572–601. <https://doi.org/10.3390/catal2040572>
26. Mir NA, Haque MM, Khan A, Umar K, Muneer M, Vijayalakshmi S (2012) Semiconductor mediated photocatalysed reaction of two selected organic compounds in aqueous suspensions of titanium dioxide. *Adv Oxid Technol* 15(2):380–391

**Publisher's Note** Springer Nature remains neutral with regard to jurisdictional claims in published maps and institutional affiliations.